Int. J. Solids Structures Vol. 30, No. 1, pp. 61–89, 1993
Printed in Great Britain.

0020–7683/93 $5.00+ .00

ADIABATIC SHEAR BAND LOCALIZATION IN ELASTIC–PLASTIC SINGLE CRYSTALS

MARIA K. DUSZEK-PERZYNA and PIOTR PERZYNA
Institute of Fundamental Technological Research, Polish Academy of Sciences,
Warsaw, Poland

(*Received* 26 *September* 1991; *in revised form* 2 *May* 1992)

Abstract—The main objective of the paper is the investigation of shear band localization criteria for finite elastic–plastic deformations of a single crystal subjected to an adiabatic process. The next objective is to focus attention on the temperature dependent plastic behaviour of the single crystal considered. A constitutive model is developed within the thermodynamic framework of the rate type covariance constitutive structure, i.e. it is invariant with respect to diffeomorphism. To achieve this aim a multiplicative decomposition of the deformation gradient is adopted and the Lie derivative is used to define all objective rates for introduced vectors and tensors. Thermomechanical couplings are investigated and a method is developed which allows us to use the standard bifurcation procedure in the examination of the adiabatic shear band localization. The general evolution equation for the Kirchhoff stress tensor is obtained. The fundamental matrix in this evolution equation describes thermomechanical couplings as well as local lattice deformation and rotation. For the particular elastic properties of the single crystal and for some simplified case of the coupling effects the criteria for adiabatic shear band localization are obtained in their exact analytical form. The influence of two important thermal effects, namely thermal expansion and thermal plastic softening on the criteria of localization is investigated. The similar influence of spatial covariance effects (which arise from the difference between the Lie derivative and the material rate of the Kirchhoff stress tensor) is also examined.

It has been shown that by incorporating the thermomechanical effects and the spatial covariance effects into a constitutive law of the elastic–plastic single crystal, the plastic hardening modulus h_{crit} at the inception of localization is in fact small but positive.

It has also been proved that this thermomechanical theory of single crystals can describe the misalignment of the shear bands from the active slip systems in the crystal's matrix. The computed critical value of the strain-hardening rate h_{crit} as well as the difference between the direction of the macroscopic shear band and the primary slip systems of the single crystal appeared to be in accord with recent experimental observations [*cf.* Chang and Asaro (1981, *Acta Metall.* **29**, 241–257) for Al–Cu single crystals and Spitzig (1981, *Acta Metall.* **29**, 1359–1377) for Fe–Ti–Mn single crystals].

1. INTRODUCTION

During the past 20 years there has been significant progress in constitutive modelling of the metallic single crystal behaviour as well as in the description of the localized deformations of ductile single crystals.

In a group of papers concerned with the description of constitutive properties of single crystals we have to mention the following: Hill (1966, 1967, 1972); Hutchinson (1970, 1976); Rice (1971); Hill and Rice (1972, 1973); Asaro and Rice (1977); Havner and Shalaby (1977); Peirce *et al.* (1982, 1983); Asaro and Needleman (1985); Iwakuma and Nemat-Nasser (1984); Nemat-Nasser and Obata (1986); Perzyma (1988); and review papers by Asaro (1983a, b).

An analysis of strain localization in ductile crystals has been presented by Rice (1977), Asaro and Rice (1977), Peirce *et al.* (1982, 1983), in review papers by Asaro (1983a, b) and very recently by Su and Lu (1991).

Experimental observations of the shear band localization in single crystals have been recently performed by Chang and Asaro (1980, 1981) and Spitzig (1981).

The paper by Asaro and Rice (1977) has clearly shown that the classical theory of crystals based on the Schmid constitutive law does not seem appropriate to explain the shear band localization phenomenon in ductile metallic single crystals.

Asaro and Rice (1977) have suggested that we "examine the possibility that localized deformation may, in some circumstances, arise for reasons other than work-softening or related degradations in strength." They have focused attention on the localization criteria

for "an assumed class of materials that essentially obey Schmid's rule but display modest departure from it." Starting with the theoretical study of localization viewed as a bifurcation from a homogeneous deformation mode to one which is concentrated in a narrow shear band they have proved that the plastic hardening rate h_{crit} at the inception of localization may be positive when there are deviations from the Schmid rule.

The second important fact of the shear band localization in ductile metallic single crystals has been recently observed by Chang and Asaro (1981) for Al–Cu single crystals and Spitzig (1981) for nitrogenated Fe–Ti–Mn single crystals and is concerned with the misalignment of the shear bands by several degrees from the active slip systems in the crystal's matrix.

To describe both experimentally observed facts, namely that the shear band localization may occur for a small positive value of the plastic hardening rate h_{crit} and that the formed shear bands are misaligned with the active slip systems in the crystal's matrix by several degrees we intend to consider the synergetic effects generated by simultaneous incorporation in the constitutive model of single crystals the spatial covariance effects and the thermomechanical couplings.

The importance of adiabatic heating effects in the explanation of localized plastic deformation in single crystals was first noticed by Chin *et al.* (1964) while the lattice stretching and rotation have been broadly investigated by Asaro and Rice (1977).

The main objective of the present paper is the investigation of shear band localization criteria for finite elastic–plastic deformations of a single crystal subjected to an adiabatic process. The next objective is to focus attention on the temperature dependent plastic behaviour of a single crystal considered.

In Section 2 the experimental observations of shear band localization in single crystals are discussed. Heuristic considerations of the different plastic localized modes and physical motivations for the present research are presented.

Section 3 is devoted to the development of a constitutive model within the thermodynamic framework of the rate type covariance constitutive structure. A notion of covariance is understood in the sense that the constitutive structure of single crystals is invariant with respect to diffeomorphisms. To achieve this aim a multiplicative decomposition of the deformation gradient is adopted and the Lie derivative is used to define all objective rates for introduced vectors and tensors. Thermomechanical couplings are investigated. Particular attention is focused on the proper description of internal heating generated by the rate of internal dissipation during the adiabatic process considered.

In Section 4 the macroscopic shear band formation during an adiabatic process for single slip is studied. The general evolution equation for the Kirchhoff stress tensor is obtained. The fundamental matrix in this evolution equation describes thermomechanical couplings as well as local lattice deformation and rotation. For the particular elastic properties of the single crystal and for some simplified case of the coupling effects the criteria for adiabatic shear band localization are obtained in exact analytical form. The influence of two important thermal effects, namely thermal expansion and thermal plastic softening on the criteria of localization is investigated. The similar influence of spatial covariance effects (which arise from the difference between the Lie derivative and the material derivative of the Kirchhoff stress tensor) is also examined.

Numerical estimations of the main effects and their comparison with available experimental results are presented in Section 5.

It has been found that the predicted by theory critical value of the strain hardening rate h_{crit} as well as the misalignment of the shear bands are in accord with recent experimental observations [*cf.* Chang and Asaro (1981) for Al–Cu single crystals and Spitzig (1981) for Fe–Ti–Mn single crystals].

Section 6 is focused on a discussion of the results obtained. The possibility of deviations from the Schmid rule of the critical resolved shear stress implied by thermomechanical coupling effects has been examined. Different plastic localization modes of single crystals have been investigated, and particular attention is focused on the description of misalignment of the shear bands from the active slip systems in the crystal's matrix.

At the end of the paper final comments are summarized.

2. EXPERIMENTAL AND PHYSICAL MOTIVATIONS

2.1. *Experimental observations of localization modes*

In 1981 two important papers appeared which reported on experimental investigations of shear band localization in single crystals, namely Chang and Asaro (1981) and Spitzig (1981).

Chang and Asaro have studied Al–2.8 wt% Cu single crystals aged to contain GP zones, θ' and θ precipitates. Uniaxial tension tests (for specimens with a 2.5 cm gauge length and a square cross-section of approx. 4×4 mm) were carried out at room temperature (298K) and at 77 and 198K. The load–engineering strain curves for three different tests are illustrated in Fig. 1. In this figure, the numbered photos correspond to the indicated points on the load–nominal strain trajectories. Just after maximum load most of the investigated crystals underwent diffuse necking. As indicated by photograph 11 in Fig. 1, for crystal 43, macroscopic shear bands soon developed within the diffusely necked region. The onset of macroscopic, shear band localization corresponds to the attainment of a critically low value of the ratio of slip plane strain hardening rate, h, to current tensile stress σ, i.e. $(h/\sigma)_{\text{crit}}$. Figure 2 shows some data obtained for the ratio $(h/\sigma)_{\text{crit}}$. The bands were not aligned with active slip systems in the crystal's matrix but were misaligned by several degrees. Figure 3 shows how the material planes of the macroscopic shear bands were inclined by a small angle to adjacent slip traces. The amount of rotation was estimated by Chang and Asaro (1981) to be 4–5°. The idea is to rotate the slip plane in the band toward the material plane of the band.

In Fig. 4 the macroscopic shearing in θ strengthened crystals is shown. After necking (and maximum load) macroscopic localized shear sets in at nearly 45° to the tensile axis on the material plane of maximum stress. In all cases fractures took place within the macroscopically localized bands (*cf.* Fig. 4). The fractures were ductile and involved void and crack initiation where shear bands intersected the free surfaces and crack growth along the bands.

It is noteworthy that Chang and Asaro (1981) found no indications of strain softening at the initiation of coarse slip bands or macroscopic shear bands, or even in fully developed macroscopic shear bands.

Spitzig (1981) performed uniaxial tension tests of nitrogenated Fe–0.19 Ti–0.39 Mn single crystals (for sheet tension specimens with a gauge length of about 1.5 cm and a cross-section of about 2.5×0.9 mm) at temperatures between 77 and 473K. He has observed that after necking begins, macroscopic localized shear bands form, with subsequent deformation occurring by localized shearing within a shear band under a decreasing load. Final separation occurred by a ductile rupture mechanism along the shear band (*cf.* Fig. 5). The onset of the localized shear bands was estimated for the ratio of the strain-hardening rate to current tensile stress $(h/\sigma)_{\text{crit}}$ to be between 0.03 and 0.06. Analysis of the localized shear bands in Fig. 6 indicates that the angle between the primary slip traces and the localized shear bands is about 5°.

2.2. *Heuristic considerations*

From the analysis of the experimental investigations of localized shearing in single crystals performed by Chang and Asaro (1981) and Spitzig (1981) we can follow the events in the order in which things naturally happen within a gauge length of the specimen during the uniaxial test.

In the first stage of the process a crystal specimen undergoes uniform extension in single slip. At the point when the load–engineering strain trajectory reaches its maximum, i.e. when the criterion for the onset of the localization by necking mode is satisfied [this is illustrated in Fig. 7(a)], a crystal specimen exhibits slight amounts of very diffuse necking. The neck is usually symmetric in shape indicating that double slip is operative within it. At this stage of the tensile process the gross plastic deformations are localized to the diffusely necked region. So, at this stage of the process the thermomechanical coupling effects begin to play a crucial role. That is why in this region of the specimen the tensile process has to be considered as *adiabatic*.

With continued extension macroscopic, adiabatic shear bands have soon developed within the diffusely necked region. In Fig. 7 this point on the load–engineering strain trajectory is marked by (b). This point (b) on the shear stress–shear strain trajectory (*cf.* Fig. 7) is found experimentally to lie on the increasing part of this curve very near to the maximum point, so that a critical value of the strain-hardening rate $h_{\text{cri}} = (\mathrm{d}\tau/\mathrm{d}\gamma)_{(b)}$ is small but positive.

It has been experimentally observed that at the inception of the macroscopic, adiabatic shear band [*cf.* Fig. 7(b)] the direction of the band is slightly different from the detected coarse slip bands or slip traces. In other words the macroscopic shear bands are not aligned with the active slip systems in the crystal's matrix but are misaligned by angle δ_b [*cf.* Fig. 7(b)].

While the tensile process is going on and is reaching point (c) on the load–nominal strain trajectory the shear band localization is developing further and the misalignment is increasing, such that $\delta_c > \delta_b$ (*cf.* Fig. 7).

To describe the main experimentally observed facts connected with the macroscopic shear band localization of single crystals, namely that the strain-hardening rate h_{cri} at the inception of shear band localization is positive and the direction of the localized shear band is misaligned by some small angle δ from the active slip system, we intend to consider the synergetic effects resulting from taking into account spatial covariance effects and thermomechanical couplings.†

This idea is justified by previous heuristic considerations as well as by the suggestion we can draw from experimental observations that the detected misalignment of the shear band direction from the active slip system is directly related to local deformation and rotation of the crystal lattice [*cf.* Chang and Asaro (1980, 1981)].

Asaro and Rice (1977) have made efforts to accomplish the same aim by introducing the possibility of deviation from the Schmid rule of a critical resolved shear stress. They have proved that the first experimentally observed fact that the strain-hardening rate h_{cri} at the inception of shear band localization is positive can be described by incorporating the non-Schmid effects into the constitutive properties of the crystal.

The main objective of the present paper is to show that both previously mentioned facts can be described by incorporating synergetic effects resulting from the simultaneous consideration of spatial covariance effects and thermomechanical couplings.

3. CONSTITUTIVE STRUCTURE FOR CRYSTALS

3.1. *Kinematics of finite deformations and fundamental definitions*

In a neighbourhood of $\mathbf{X}$, i.e. $\mathcal{N}(\mathbf{X})$ for every $\mathbf{X} \in \mathcal{B}$ we consider the local multiplicative decomposition of the deformation gradient [*cf.* Lee (1969)]

$$\mathbf{F} = \mathbf{F}^{\mathrm{e}} \cdot \mathbf{F}^{\mathrm{p}}, \tag{1}$$

where $(\mathbf{F}^{\mathrm{e}})^{-1}$ is the deformation gradient that releases elastically the stress on the neighbourhood $\mathcal{N}(\mathbf{X})$ in the current configuration of the crystal.

It is understood that $\mathbf{F}^{\mathrm{e}}$ is the lattice contribution to $\mathbf{F}$, and is associated with stretching and rotation of the lattice, $\mathbf{F}^{\mathrm{p}}$ describes the deformation solely due to plastic shearing on crystallographic slip systems.

A particular slip system α is specified by the slip vectors $\mathbf{s}_0^{(\alpha)}$, $\mathbf{m}_0^{(\alpha)}$, where $\mathbf{s}_0^{(\alpha)}$ gives the slip direction and $\mathbf{m}_0^{(\alpha)}$ is the slip plane normal. The vectors $\mathbf{s}_0^{(\alpha)}$ and $\mathbf{m}_0^{(\alpha)}$ in the undeformed lattice are taken to be orthonormal. As the crystal deforms the vectors $\mathbf{s}^{(\alpha)}$ and $\mathbf{m}^{(\alpha)}$ are

† Spatial covariance effects are generated by the difference between the Lie derivative and the material derivative of vectors and tensors involved in the description.

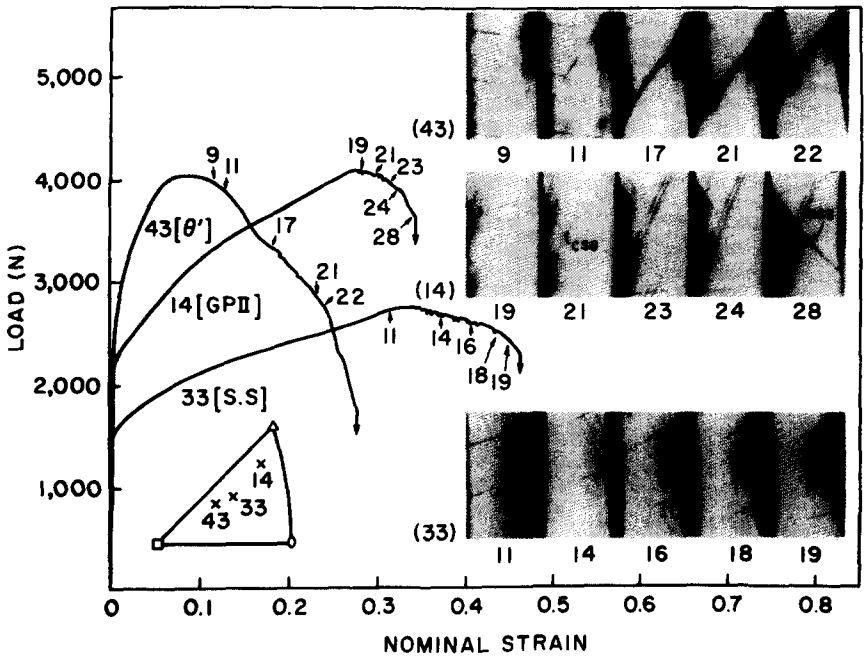

Fig. 1. Load versus engineering strain curves for various ageing treatments. Numbered photos correspond to the indicated points on the load–strain band [after Chang and Asaro (1981)].

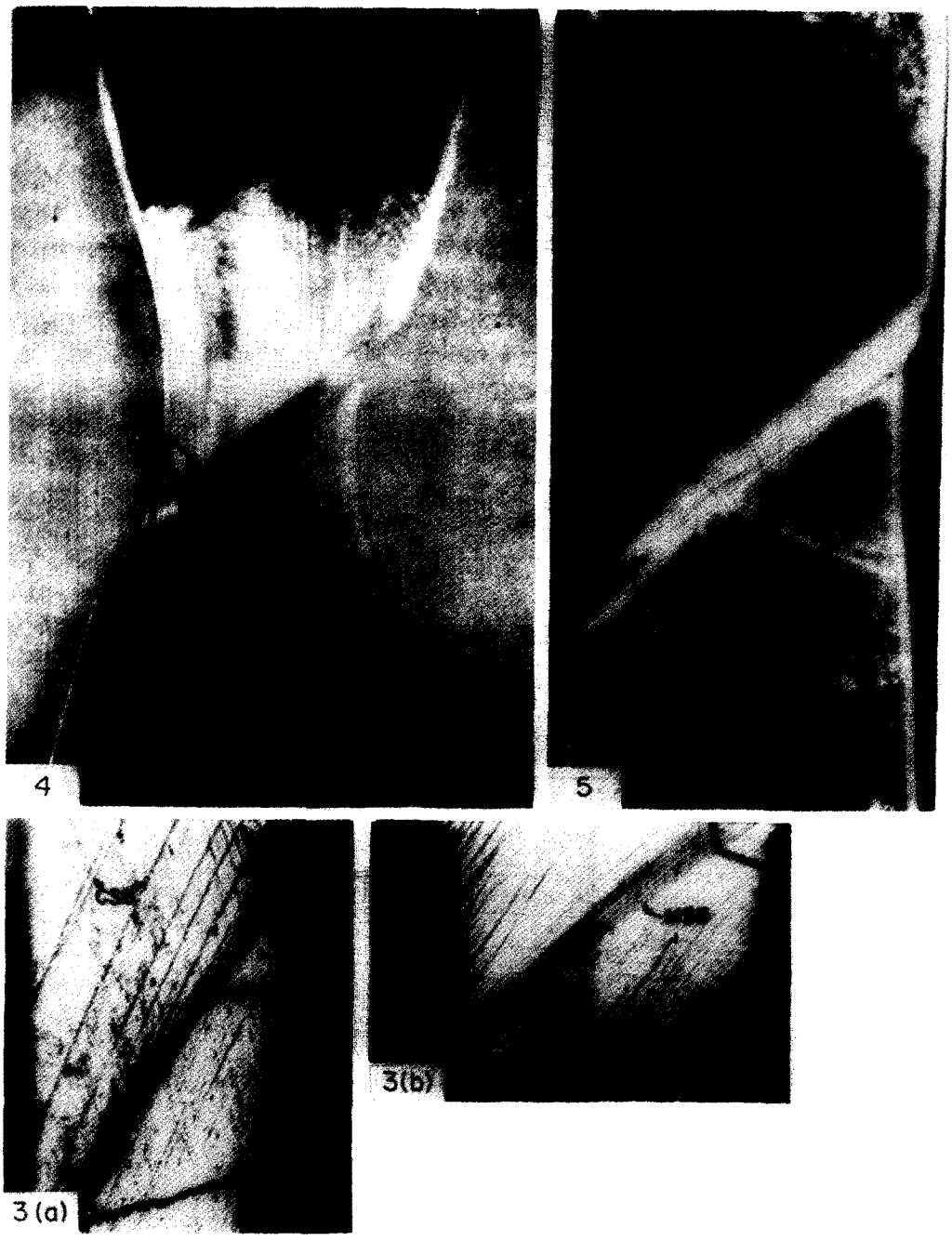

Fig. 3. Coarse slip bands (CSB) and macroscopic shear bands (MSB) in (a) GPII tested at 77K and (b) a θ' strengthened crystal tested at 298K. Note the orientation difference between CSBs and MSBs in (a), CBSs are closely aligned with the active slip systems [after Chang and Asaro (1981)].

Fig. 4. Macroscopic shearing in θ strengthened crystals. After necking (and load maximum) macroscopic localized shear sets in at nearly 45° to the tensile axis on the material plane of maximum shear [after Chang and Asaro (1981)].

Fig. 5. Propagation of localizaed shear in nitrogenated Fe–Ti–Mn crystal of orientation D deformed at 295K, 40% decrease in load from maximum load [after Spitzig (1981)].

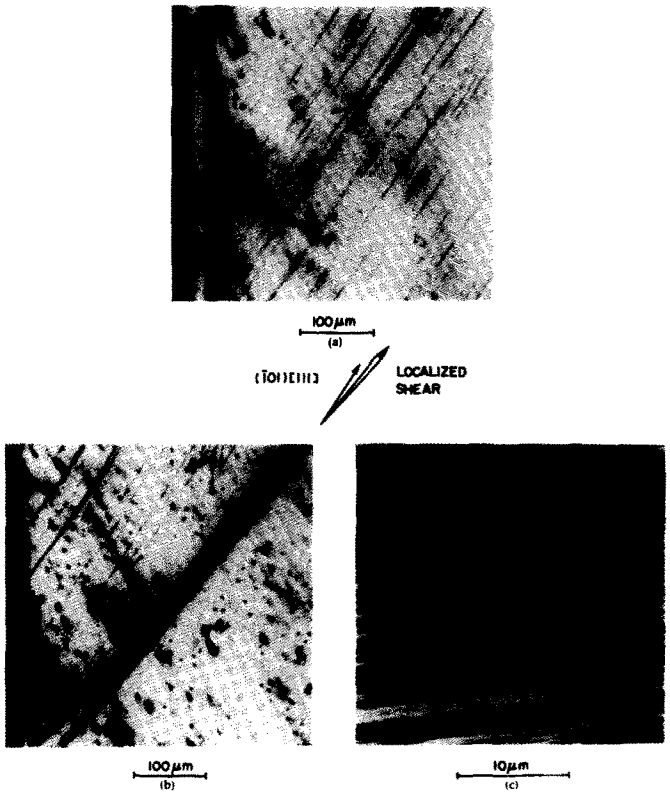

Fig. 6. Slip traces and localized shear on the surface of nitrogenated Fe–Ti–Mn crystal of orientation *D* deformed at 295K: (a) initial deformation until necking began, (b) subsequent deformation after removal of neck and localized shear bands from initial deformation, (c) slip traces within localized shear band in (b) [after Spitzig (1981)].

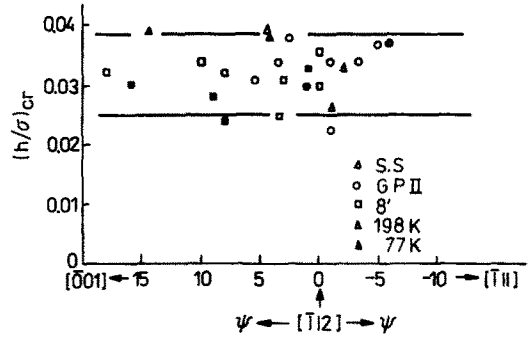

Fig. 2. Critical ratio $(h/\sigma)_{crit}$ versus ψ, the angle between the tensile axis and [T12] for various ageing treatments [after Chang and Asaro (1981)].

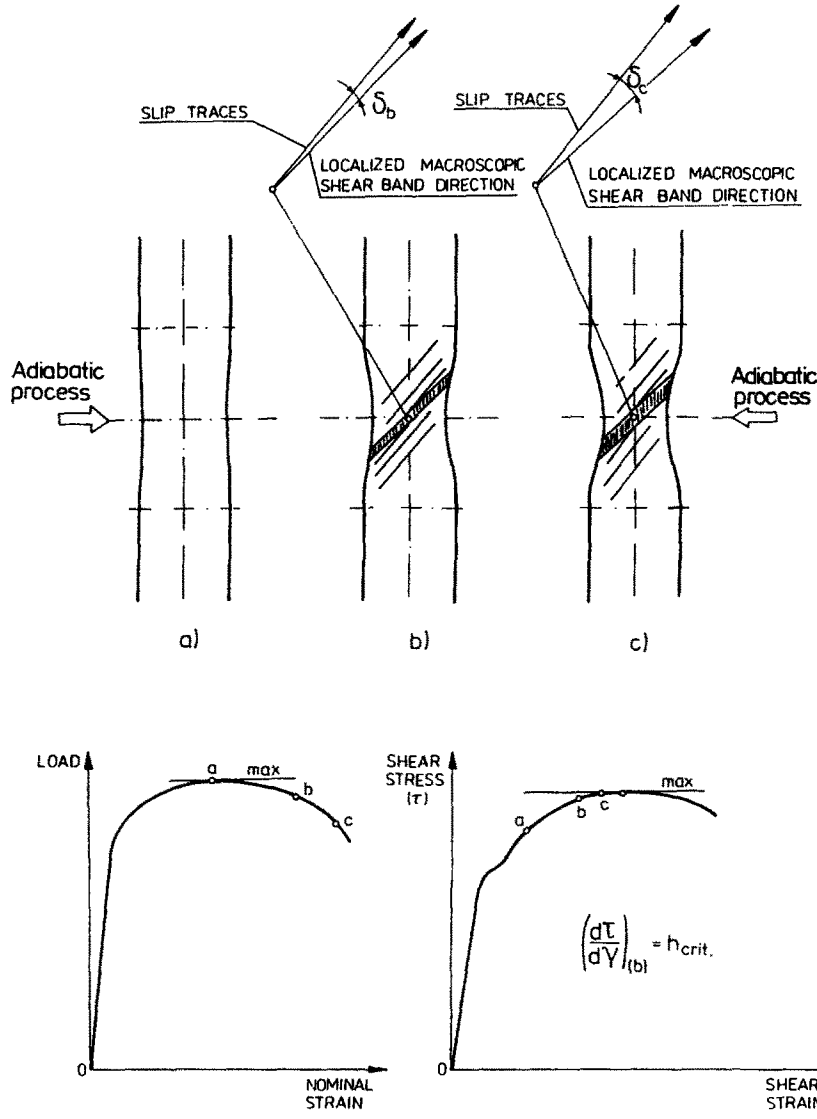

Fig. 7. Heuristic considerations of the shear band localization in single crystals: (a) initiation of diffuse necking; (b) inception of the shear band loclization; (c) advanced shear band localization.

stretched and rotated according to $\mathbf{F}^e$. In the deformed lattice we have

$$\mathbf{s}^{(\alpha)} = \mathbf{F}^e \cdot \mathbf{s}_0^{(\alpha)}, \quad \mathbf{m}^{(\alpha)} = \mathbf{m}_0^{(\alpha)} \cdot (\mathbf{F}^e)^{-1}. \tag{2}$$

Let us define the Eulerian velocity gradient $\mathbf{l} = (\partial \mathbf{v}/\partial \mathbf{x})$ in the current state of the crystal by

$$\mathbf{l} = \dot{\mathbf{F}} \cdot \mathbf{F}^{-1} = \dot{\mathbf{F}}^e \cdot \mathbf{F}^{e\,-1} + \mathbf{F}^e \cdot \dot{\mathbf{F}}^p \cdot \mathbf{F}^{p\,-1} \cdot \mathbf{F}^{e\,-1} \tag{3}$$

and postulate for the plastic part

$$\mathbf{l}^p = \dot{\mathbf{F}} \cdot \mathbf{F}^{-1} - \dot{\mathbf{F}}^e \cdot \mathbf{F}^{e\,-1} = \mathbf{F}^e \cdot \dot{\mathbf{F}}^p \cdot \mathbf{F}^{p\,-1} \cdot \mathbf{F}^{e\,-1} = \sum_{\alpha=1}^{n} \mathbf{s}^{(\alpha)} \mathbf{m}^{(\alpha)} \dot{\gamma}^{(\alpha)}, \tag{4}$$

where $\dot{\gamma}^{(\alpha)}$ is the rate of shearing on slip system α.

Then instead of (3) we can write

$$\mathbf{l} = \mathbf{l}^e + \mathbf{l}^p = \mathbf{d} + \boldsymbol{\omega} = \mathbf{d}^e + \boldsymbol{\omega}^e + \mathbf{d}^p + \boldsymbol{\omega}^p, \tag{5}$$

where $\mathbf{d}$ is the symmetric rate of the stretching tensor and $\boldsymbol{\omega}$ is the anti-symmetric spin rate. The elastic rates of stretching and spin $\mathbf{d}^e$ and $\boldsymbol{\omega}^e$ are the symmetric and anti-symmetric parts of $\dot{\mathbf{F}}^e \cdot \mathbf{F}^{e\,-1}$, respectively. The plastic parts of the rate of stretching and spin are determined by the relations:

$$\mathbf{d}^p = \sum_{\alpha=1}^{n} \dot{\gamma}^{(\alpha)} \mathbf{N}^{(\alpha)}, \quad \boldsymbol{\omega}^p = \sum_{\alpha=1}^{n} \dot{\gamma}^{(\alpha)} \mathbf{W}^{(\alpha)}, \tag{6}$$

where

$$\mathbf{N}^{(\alpha)} = \tfrac{1}{2}[\mathbf{s}^{(\alpha)} \mathbf{m}^{(\alpha)} + \mathbf{m}^{(\alpha)} \mathbf{s}^{(\alpha)}], \quad \mathbf{W}^{(\alpha)} = \tfrac{1}{2}[\mathbf{s}^{(\alpha)} \mathbf{m}^{(\alpha)} - \mathbf{m}^{(\alpha)} \mathbf{s}^{(\alpha)}]. \tag{7}$$

On the other hand if $\mathbf{e}$ and $\mathbf{e}^e$ are the Eulerian strain tensors then by definition we can specify the plastic strain tensor $\mathbf{e}^p$ as

$$\mathbf{e}^p = \mathbf{e} - \mathbf{e}^e. \tag{8}$$

Introducing the Lie derivative of a spatial tensor field with respect to the velocity field $\mathbf{v}$, denoted by $L_{\mathbf{v}}$†, we can define the rates of deformation as follows:

$$\mathbf{d} = L_{\mathbf{v}} \mathbf{e}, \quad \mathbf{d}^e = L_{\mathbf{v}} \mathbf{e}^e, \quad \mathbf{d}^p = L_{\mathbf{v}} \mathbf{e}^p. \tag{9}$$

We have again

$$\mathbf{d} = \mathbf{d}^e + \mathbf{d}^p. \tag{10}$$

Let $\boldsymbol{\tau}$ denote the Kirchhoff stress tensor, and take the rate of stress working per unit reference volume

$$\boldsymbol{\tau} : \mathbf{d} = \boldsymbol{\tau} : \mathbf{d}^e + \boldsymbol{\tau} : \mathbf{d}^p = \boldsymbol{\tau} : \mathbf{d}^e + \sum_{\alpha=1}^{n} \tau^{(\alpha)} \dot{\gamma}^{(\alpha)}, \tag{11}$$

where

$$\tau^{(\alpha)} = \boldsymbol{\tau} : \mathbf{N}^{(\alpha)} = \mathbf{s}^{(\alpha)} \cdot \boldsymbol{\tau} \cdot \mathbf{m}^{(\alpha)} \tag{12}$$

is the Schmid resolved shear stress on the slip system α.

† For precise definition of the Lie derivative and its geometrical interpretation please consult Abraham *et al.* (1988). Application of the Lie derivative to continuum mechanics may be found in Marsden and Hughes (1983) and Simo (1988).

The Lie derivative of the contravariant representation of the Kirchhoff stress tensor τ gives‡

$$(L_v\tau)^{ab} = \frac{\partial \tau^{ab}}{\partial t} + \frac{\partial \tau^{ab}}{\partial x^c} v^c - \tau^{cb}\frac{\partial v^a}{\partial x^c} - \tau^{ac}\frac{\partial v^b}{\partial x^c}. \tag{13}$$

It is important to stress that any possible objective rate of the stress tensor is a particular case of the Lie derivative [*cf.* Marsden and Hughes (1983)].

The Zaremba–Jaumann stress rate or the co-rotated derivative of the Kirchhoff stress tensor τ is related to the Lie derivative given by (13) as follows:

$$\overset{\nabla}{\tau} = L_v\tau + \mathbf{d}\cdot\tau + \tau\cdot\mathbf{d}. \tag{14}$$

It is noteworthy that there are two levels of objectivity for the constitutive structure:

(i) *Frame invariance.* The constitutive structure should be invariant with respect to superposed rigid body motion [*cf.* Truesdell and Noll (1965)].

(ii) *Spatial covariance.* The constitutive structure should be invariant with respect to diffeomorphism [*cf.* Marsden and Hughes (1983)].

In further considerations we shall take advantage of both notions of objectivity.

3.2. *Constitutive postulates*

For rate independent behaviour of single crystals the constitutive assumptions have been introduced by Schmid (1924).

The Schmid resolved shear stress (12) determines the slip behaviour as follows. When $\tau^{(\alpha)}$ reaches a critical value $\tau_c^{(\alpha)}$, i.e.

$$\tau^{(\alpha)} = \tau_c^{(\alpha)}, \quad \alpha = 1, \ldots, n, \tag{15}$$

slip initiates on system α.

Similarly as have been assumed by Pierce *et al.* (1982) to deal with the possibility that slip may be either forward to backward according to whether $\tau^{(\alpha)}$ is positive or negative, $(\mathbf{s}^{(\alpha)}, \mathbf{m}^{(\alpha)})$ and $(-\mathbf{s}^{(\alpha)}, \mathbf{m}^{(\alpha)})$ are considered as separate slip systems on each of which only positive slip is allowed.

After initial yield, slip continues on system α if the resolved shear stress $\tau^{(\alpha)}$ on that system keeps pace with the flow stress.

The work hardening–softening law is postulated in the form

$$\tau_c^{(\alpha)} = \tau_c^{(\alpha)}(\gamma, \vartheta), \tag{16}$$

where

$$\gamma = \sum_{\alpha=1}^{n} \gamma^{(\alpha)}, \tag{17}$$

then $\tau_c^{(\alpha)}$ do not play the role of the internal state variables.

For an active system β we have

$$\tau^{(\beta)} = \tau_c^{(\beta)}(\gamma, \vartheta), \quad \dot{\gamma}^{(\beta)} > 0, \tag{18}$$

while for an inactive system

‡ It is noteworthy that (13) defines the Oldroyd rate of the Kirchhoff stress tensor τ [*cf.* Oldroyd (1950)].

$$\tau^{(\alpha)} \leqslant \tau_c^{(\alpha)}(\gamma, \vartheta), \quad \dot{\gamma}^{(\alpha)} = 0. \tag{19}$$

3.3. *Thermodynamic restrictions*

Consider the balance principles as follows:

(i) *Conservation of mass.* Denote by $\rho(\mathbf{x}, t)$ the mass denisty (in spatial coordinates). A function $\rho(\mathbf{x}, t)$ is said to obey conservation of mass if

$$\dot{\rho} + \rho \operatorname{div} \mathbf{v} = 0 \tag{20}$$

or

$$\rho(\mathbf{x}, t) J(\mathbf{X}, t) = \rho_{\mathrm{Ref}}(\mathbf{X}), \tag{21}$$

where $J(\mathbf{X}, t)$ denotes the Jacobian.

(ii) *Balance of momentum.* Assume that conservation of mass and balance of momentum hold. If there is no external body force field, then

$$\rho \dot{\mathbf{v}} = \operatorname{div} \boldsymbol{\sigma}, \tag{22}$$

where $\boldsymbol{\sigma} = J^{-1} \boldsymbol{\tau}$ is the Cauchy stress tensor.

(iii) *Balance of moment of momentum.* Let conservation of mass and balance of momentum hold. Then balance of moment of momentum holds if and only if $\boldsymbol{\tau}$ is symmetric.

(iv) *Balance of energy.* Assume the following balance principles hold: conservation of mass, balance of momentum, balance of moment of momentum and balance of energy. If there is no external heat supply then

$$\rho(\dot{\psi} + \vartheta \dot{\eta} + \eta \dot{\vartheta}) + \operatorname{div} \mathbf{q} = \frac{\rho}{\rho_{\mathrm{Ref}}} \boldsymbol{\tau} : \mathbf{d}, \tag{23}$$

where η denotes the specific (per unit mass) entropy, ψ the free energy and $\mathbf{q}$ is the heat vector field.

(v) *Entropy production inequality.* Assume conservation of mass, balance of momentum, moment of momentum, energy and the entropy production inequality hold. Then the reduced dissipation inequality is satisfied:

$$\frac{1}{\rho_{\mathrm{Ref}}} \boldsymbol{\tau} : \mathbf{d} - (\eta \dot{\vartheta} + \dot{\psi}) - \frac{1}{\rho \vartheta} \mathbf{q} \cdot \operatorname{grad} \vartheta \geqslant 0. \tag{24}$$

Now we introduce the two fundamental postulates:

(i) *Existence of the free energy function.* It is assumed that the free energy function is given by

$$\psi = \hat{\psi}(\mathbf{e}, \mathbf{F}, \vartheta; \gamma^{(\alpha)}). \tag{25}$$

(ii) *The axiom of entropy production.* For any regular motion of crystal (denoted by $\mathscr{B}$) the constitutive functions are assumed to satisfy the reduced dissipation inequality (24).

Then the constitutive assumption (25) and the evolution equation for $\gamma^{(\alpha)}$ [*cf.* eqn (18)]

$$\dot{\gamma}^{(\alpha)} = \sum_{\beta=1}^{n} \hat{h}_{\alpha\beta}^{-1} \dot{\tau}^{(\beta)} + \pi^{(\alpha)} \dot{\vartheta}, \tag{26}$$

where

$$\hat{h}_{\alpha\beta} = \frac{\partial \tau_c^{(\alpha)}}{\partial \gamma^{(\beta)}} \quad \text{and} \quad \pi^{(\alpha)} = -\sum_{\beta=1}^{n} \frac{\partial \tau_c^{(\beta)}}{\partial \vartheta}(\hat{h}_{\alpha\beta}), \tag{27}$$

together with the reduced dissipation inequality (24) lead to the results as follows:

$$\tau = \rho_{\mathrm{Ref}} \frac{\partial \hat{\psi}}{\partial \mathbf{e}}, \quad \eta = -\frac{\partial \hat{\psi}}{\partial \vartheta},$$

$$\vartheta \hat{i} - \frac{1}{\rho \vartheta} \mathbf{q} \cdot \operatorname{grad} \vartheta \geqslant 0, \tag{28}$$

where

$$\vartheta \hat{i} = -\sum_{\alpha=1}^{n} \frac{\partial \hat{\psi}}{\partial \gamma^{(\alpha)}} \dot{\gamma}^{(\alpha)} \tag{29}$$

denotes the rate of the internal dissipation.

Introducing the denotation

$$\chi \tau^{(\alpha)} = -\rho \frac{\partial \hat{\psi}}{\partial \gamma^{(\alpha)}}, \tag{30}$$

we have

$$\vartheta \hat{i} = \chi \sum_{\alpha=1}^{n} \frac{1}{\rho} \tau^{(\alpha)} \dot{\gamma}^{(\alpha)}. \tag{31}$$

The coefficient χ is determined from the equation

$$\chi \rho_{\mathrm{Ref}} \frac{\partial \hat{\psi}}{\partial e} : \mathbf{N}^{(\alpha)} = -\rho \frac{\partial \hat{\psi}}{\partial \gamma^{(\alpha)}}. \tag{32}$$

3.4. *Rate type constitutive relation*

This consideration follows the formulation of the rate type constitutive relation presented by Hill and Rice (1972, 1973) [*cf.* also Perzyna (1990)].

The basic assumption is that the response of the materials of single crystals is always of Green type, i.e. that the free energy function exists and is given in the form (25).

Let us assume that the thermodynamic restrictions give the results presented in the form (28). We say that a set of the internal state variables $\gamma^{(\alpha)}$ ($\alpha = 1, \ldots, n$), together with the evolution equations (26) and the initial values for $\gamma^{(\alpha)}$, describes the prior history of inelastic deformation of the single crystal.

Let us consider purely elastic deformation–temperature process. For such a process let us operate on the stress relation (28_1) with the Lie derivative. The result of this operation is as follows

$$\overset{\mathrm{el}}{(\overline{L_v \tau})} = \mathscr{L}^{\mathrm{e}} \cdot \mathbf{d}^{\mathrm{e}} - \boldsymbol{\theta} \mathbf{z} \dot{\vartheta}, \tag{33}$$

where

$$\overset{\mathrm{el}}{(\overline{L_v \tau})}^{ab} = \dot{\tau}^{ab} - \tau^{ac}(d^{\mathrm{e}}_{dc} + \omega^{\mathrm{e}}_{dc}) g^{db} - \tau^{cb}(d^{\mathrm{e}}_{dc} + \omega^{\mathrm{e}}_{dc}) g^{ad},$$

$$\mathscr{L}^{\mathrm{e}} = \rho_{\mathrm{Ref}} \frac{\partial^2 \hat{\psi}}{\partial \mathbf{e}^2}, \quad \boldsymbol{\theta} \mathbf{z} = -\rho_{\mathrm{Ref}} \frac{\partial^2 \psi}{\partial \mathbf{e} \, \partial \vartheta} \tag{34}$$

and θ denotes the thermal expansion coefficient.

On the other hand for general deformation–temperature process (when the internal state variables $\gamma^{(\alpha)}$, $\alpha = 1, \ldots, n$ vary) we have

$$(L_v\boldsymbol{\tau})^{ab} = \dot{\tau}^{ab} - \tau^{ac}(d_{dc}+\omega_{dc})g^{db} - \tau^{cb}(d_{dc}+\omega_{dc})g^{ad}. \tag{35}$$

Introducing the denotation

$$\mathbf{b}^{(\alpha)} = (\mathbf{N}^{(\alpha)}+\mathbf{W}^{(\alpha)})\cdot\boldsymbol{\tau}+\boldsymbol{\tau}\cdot(\mathbf{N}^{(\alpha)}-\mathbf{W}^{(\alpha)}) \tag{36}$$

we finally have the resulting constitutive law of the rate type in the form†

$$L_v\boldsymbol{\tau} = \mathscr{L}^e\cdot\mathbf{d} - \sum_{\alpha=1}^{n}[\mathscr{L}^e\cdot\mathbf{N}^{(\alpha)}+\mathbf{b}^{(\alpha)}]\dot{\gamma}^{(\alpha)} - \theta\mathbf{z}\dot{\vartheta}. \tag{37}$$

The result obtained in the form (37) has a similar shape to the rate equation formulated by Hill and Rice (1972) [*cf.* also the recent paper by Perzyna (1991)]. The main difference is in the definition of the Kirchhoff stress rate and of course in the additional thermal expansion term. Hill and Rice (1972) used the Zaremba–Jaumann rate, while in the present paper [as well as in Perzyna (1990)] the Lie derivative of the Kirchhoff stress tensor has been used. That is why the term proportional to $\mathbf{b}^{(\alpha)}$, which represents the stiffening of the lattice due to microscopic phenomena associated with continued slipping depends in our case on the rate of plastic spin as well as on the rate of plastic deformation, while in the Hill and Rice paper (1972) a similar term proportional to

$$\boldsymbol{\beta}^{(\alpha)} = \mathbf{W}^{(\alpha)}\cdot\boldsymbol{\tau} - \boldsymbol{\tau}\cdot\mathbf{W}^{(\alpha)} \tag{38}$$

depends on the rate of plastic spin only.

3.5. *Thermomechanical couplings*‡

Substituting $\dot{\psi}$ into the energy balance equation (23) and taking advantage of the results (28) gives

$$\rho\vartheta\dot{\eta} = -\operatorname{div}\mathbf{q}+\rho\vartheta\hat{l}. \tag{39}$$

Operating on the entropy relation (28_2) with the Lie derivative and substituting the result together with the Fourier constitutive law for the heat vector field

$$\mathbf{q} = -k\operatorname{grad}\vartheta, \tag{40}$$

where k is the conductivity coefficient, into (39) we obtain the heat conduction equation in the following form:

$$\rho c_p\dot{\vartheta} = \operatorname{div}(k\operatorname{grad}\vartheta)+\vartheta\frac{\rho}{\rho_{\mathrm{Ref}}}\frac{\partial\boldsymbol{\tau}}{\partial\vartheta}:\mathbf{d}+\chi\sum_{\alpha=1}^{n}\tau^{(\alpha)}\dot{\gamma}^{(\alpha)}+\rho\vartheta\sum_{\alpha=1}^{n}\frac{\partial^2\psi}{\partial\vartheta\,\partial\gamma^{(\alpha)}}\dot{\gamma}^{(\alpha)}, \tag{41}$$

where

$$c_p = -\vartheta\frac{\partial^2\psi}{\partial\vartheta^2} \tag{42}$$

denotes the specific heat.

In view of (31) the term

$$\chi\sum_{\alpha=1}^{n}\tau^{(\alpha)}\dot{\gamma}^{(\alpha)}$$

† By performing a Legendre transformation it is possible to obtain the inverse form of the rate type constitutive relation (37).

‡ It is noteworthy that in the description of thermomechanical couplings (Section 3.5) and the adiabatic process (Section 3.6) for a single crystal we take advantage of a similar procedure as has been developed for polycrystalline elastic–plastic solids by Duszek and Perzyna (1991) [*cf.* also Perzyna (1990)].

on the right-hand side of eqn (41) represents the internal heating generated by the rate of internal dissipation. This term describes the main contribution to the thermomechanical coupling phenomena.

Beside this main term there appears two additional terms responsible for the cross coupling effects, namely the term proportional to

$$\frac{\partial \boldsymbol{\tau}}{\partial \vartheta} : d$$

caused by the dependence of the stress tensor on temperature, and the term proportional to

$$\sum_{\alpha=1}^{n} \frac{\partial^2 \psi}{\partial \vartheta \, \partial \gamma^{(\alpha)}} \dot{\gamma}^{(\alpha)}$$

implied by the dependence of the generalized forces conjugate to the internal state variables $\gamma^{(\alpha)}$ on temperature.

The first of these two additional terms does not have a dissipative character, while the second is very dissipative in its nature.

3.6. *Adiabatic process*

The thermodynamic process is assumed to be adiabatic, i.e.

$$\mathbf{q} = 0. \tag{43}$$

Then the term div (k grad ϑ) in the heat conduction equation (41) vanishes.

The second and fourth terms on the right-hand side of eqn (41) (which represent the cross coupling effects) influence the evolution of temperature through the second order terms when compared with the internal dissipation term. Their contribution to internal heating during the adiabatic process considered is small. This suggests that these two terms can be neglected in some considerations like the adiabatic shear band formation in the single crystal.

So, it is reasonable to consider the evolution equation for temperature in the form

$$\rho c_p \dot{\vartheta} = \chi \sum_{\alpha=1}^{n} \tau^{(\alpha)} \dot{\gamma}^{(\alpha)}, \tag{44}$$

where the coefficient χ is determined by eqn (32).

4. MACROSCOPIC SHEAR BAND FORMATION

4.1. *Adiabatic process for single slip*

Let us consider only single slip for the adiabatic process. Then we have [*cf.* eqn (15)]

$$\tau = \tau_c(\gamma, \vartheta). \tag{45}$$

Differentiation of eqn (45) with respect to time gives†

† For single slip in the adiabatic process by using the evolution equation for temperature

$$\dot{\vartheta} = \frac{\chi}{\rho c_p} \tau \dot{\gamma}$$

we can write the rate equation (46) as follows:

$$\dot{\gamma} = \frac{1}{h^{\text{adiabatic}}} \dot{\tau},$$

where

$$h^{\text{adiabatic}} = h + \chi \frac{\tau}{\rho c_p} \left(\frac{\partial \tau_c}{\partial \vartheta} \right) = h + h^{\text{thermal}}.$$

$$\dot{\gamma} = \frac{1}{h}\dot{\tau} + \pi\dot{\vartheta}, \tag{46}$$

where the notations [*cf.* eqn (27)]

$$h = \frac{\partial \tau_c}{\partial \gamma}, \quad \pi = -\frac{1}{h}\frac{\partial \tau_c}{\partial \vartheta}, \tag{47}$$

are introduced.

For single slip we can write

$$\tau = \tau^{ab} s_b m_a = m_a \tau^a_b s^b. \tag{48}$$

Operating on (48) with the Lie derivative $(\overset{\text{el}}{\overline{L_v}})$, i.e. taking the rate of change seen by an observer who stretches and rotates with the crystal lattice, we obtain

$$\begin{aligned} \dot{\tau} &= (\overset{\text{el}}{\overline{L_v \tau}})^{ab} s_b m_a + \tau^{ab} (\overset{\text{el}}{\overline{L_v \mathbf{s}}})_b m_a + \tau^{ab} s_b (\overset{\text{el}}{\overline{L_v \mathbf{m}}})_a \\ &= (\overset{\text{el}}{\overline{L_v \mathbf{m}}})_a \tau^a_b s^b + m_a (\overset{\text{el}}{\overline{L_v \tau}})^a_b s^b + m_a \tau^a_b (\overset{\text{el}}{\overline{L_v \mathbf{s}}})^b. \end{aligned} \tag{49}$$

From (49) we have

$$\dot{\tau} = (\overset{\text{el}}{\overline{L_v \boldsymbol{\tau}}}) : \mathbf{N} + 2\boldsymbol{\tau} \cdot (\mathbf{N} + \mathbf{W}) \cdot \mathbf{g} \cdot \mathbf{d}^e \tag{50}$$

and

$$\dot{\tau} = m_a (\overset{\text{el}}{\overline{L_v \boldsymbol{\tau}}})^a_b s^b. \tag{51}$$

It is noteworthy that the relation (51) has a very simple form. It can be compared with the result (50) of Hill and Rice (1972) and with eqn (2.16_3) in Asaro and Rice (1977).

Substituting the rate relation for the elastic range (33) into (50) we have

$$\dot{\tau} = [\mathscr{L}^e : \mathbf{N} + \mathbf{b}] : (\mathbf{d} - \mathbf{d}^p) - \theta \mathbf{z} : \mathbf{N}\dot{\vartheta}. \tag{52}$$

Replacing $\dot{\tau}$ in (46) by (52) yields:

$$\dot{\gamma} = \frac{1}{h}[\mathscr{L}^e : \mathbf{N} + \mathbf{b}] : (\mathbf{d} - \mathbf{d}^p) - \frac{1}{h}\theta \mathbf{z} : \mathbf{N}\dot{\vartheta} + \pi\dot{\vartheta}. \tag{53}$$

Let us take advantage of the rate equation for the Kirchhoff stress tensor (46), the evolution equation for temperature (44) and the plastic strain rate (6) for single slip, i.e.

$$\begin{aligned} \mathsf{L}_v \boldsymbol{\tau} &= \mathscr{L}^e : \mathbf{d} - \theta \mathbf{z}\dot{\vartheta} - (\mathscr{L}^e : \mathbf{N} + \mathbf{b})\dot{\gamma}, \\ \rho c_p \dot{\vartheta} &= \chi \tau \dot{\gamma}, \\ \mathbf{d}^p &= \mathbf{N}\dot{\gamma}. \end{aligned} \tag{54}$$

Using (54_3) in (53) gives

$$\dot{\gamma} = \frac{\mathbf{Q}^* : \mathbf{d}}{h - \Pi\tau : \mathbf{N} + \left(\mathbf{Q}^* + \Theta \frac{\mathbf{z}}{\mu}\tau : \mathbf{N}\right) : \mathbf{N}}, \tag{55}$$

with the denotations as follows:

$$\begin{aligned} \mathbf{Q}^* &= \mathscr{L}^e : \mathbf{N} + \mathbf{b}, \\ \Theta &= \frac{\chi\theta}{\rho c_p}\mu, \\ \Pi &= \frac{\chi}{\rho c_p} h\pi = -\frac{\chi}{\rho c_p}\frac{\partial \tau_c}{\partial \vartheta}. \end{aligned} \tag{56}$$

Eliminating $\dot{\gamma}$ and $\dot{\vartheta}$ from $(54_{1,2})$ and (55) we obtain the fundamental rate equation for the Kirchhoff stress tensor τ in the following form:

$$\mathsf{L}_v \tau = \mathbb{L} : \mathbf{d}, \tag{57}$$

where

$$\mathbb{L} = \left[\mathscr{L}^e - \frac{\left(\mathbf{Q}^* + \Theta \frac{\mathbf{z}}{\mu}\tau : \mathbf{N}\right)\mathbf{Q}^*}{h - \Pi\tau : \mathbf{N} + \left(\mathbf{Q}^* + \Theta \frac{\mathbf{z}}{\mu}\tau : \mathbf{N}\right) : \mathbf{N}} \right]. \tag{58}$$

It is noteworthy that the second order tensor $\mathbf{Q}^*$ is responsible for the elastic–plastic properties of the crystal while the scalar coefficients Θ and Π describe the thermal expansion and thermal plastic softening effects, respectively, and μ denotes the elastic shear modulus.

If the Zaremba–Jaumann rate instead of the Lie derivative is used then we arrive at the rate equation

$$\overset{\nabla}{\tau} = \mathbb{L}^{\#} : \mathbf{d}, \tag{59}$$

where

$$\mathbb{L}^{\#} = \left[\mathscr{L}^e - \frac{\left(\mathbf{Q}^{\#} + \Theta \frac{\mathbf{z}}{\mu}\tau : \mathbf{N}\right)\mathbf{Q}^{\#}}{h - \Pi\tau : \mathbf{N} + \left(\mathbf{Q}^{\#} + \Theta \frac{\mathbf{z}}{\mu}\tau : \mathbf{N}\right) : \mathbf{N}} \right], \tag{60}$$

and

$$\mathbf{Q}^{\#} = \mathscr{L}^e : \mathbf{N} + \boldsymbol{\beta}. \tag{61}$$

Assuming an isothermal process, i.e.

$$\vartheta = \text{const.}, \tag{62}$$

then the fundamental rate equation (59) reduces to

$$\overset{\nabla}{\tau} = \mathbb{L}^0 : \mathbf{d}, \tag{63}$$

where

$$\mathbb{L}^0 = \left[\mathscr{L}^e - \frac{\mathbf{Q}^{\#}\mathbf{Q}^{\#}}{h+\mathbf{Q}^{\#}:\mathbf{N}}\right]. \tag{64}$$

The results (63)–(64) are the same as have been obtained by Asaro and Rice (1977) [*cf.* eqn (2.24) in their paper] provided their tensor $\boldsymbol{\alpha}$, caused by non-Schmid effects, is neglected.

It is important to point out here that the Lie derivative description of the thermomechanical properties of the single crystal, in the form of the rate type equation for the Kirchhoff stress tensor τ (57) with the fundamental matrix given by (58) is invariant with respect to diffeomorphism while the Zaremba–Jaumann rate description (59)–(60), is invariant with respect to superposed rigid body motion.

In other words the formulation (57)–(58) furnishes the single crystal considered with the spatial covariance constitutive structure while (59)–(60) leads to frame invariance objectivity.

4.2. *Shear band localization criteria*

Let us introduce the Cartesian coordinate system $\{x^r\}$ in such a way that the coordinates x_1, x_2, x_3 are aligned with unit vectors of the crystal slip system **s**, **m**, **z**, respectively.

To investigate the criteria for the adiabatic shear band localization we have to consider the conditions as follows:

(i) the kinematic restriction:

$$\Delta\left(\frac{\partial v_i}{\partial x^j}\right) = k_i n_j, \tag{65}$$

where Δ denotes the jump of the function in brackets, i.e. it defines the difference between the velocity gradient inside the band from that outside and **n** is a unit normal to a thin planar band while the magnitude of jump **k** is a function of distance across the band $(\mathbf{n}\cdot\mathbf{x})$ only, and is zero outside;

(ii) the equilibrium requirement that the traction rate be continuous across the band, i.e.

$$\mathbf{n}\cdot\Delta(\dot{\boldsymbol{\sigma}}) = 0. \tag{66}$$

For the assumption that the reference state coincides, instantaneously, with the current state we have:

$$\begin{aligned}(\mathsf{L}_v\tau)^{ij} &= \dot{\tau}^{ij} - \tau^{ik}(d_{rk}+\omega_{rk})g^{rj} - \tau^{kj}(d_{rk}+\omega_{rk})g^{ri}\\ &= \dot{\sigma}^{ij} + \tau^{ij}d_{kl}g^{kl} - \tau^{ik}(d_{rk}+\omega_{rk})g^{rj} - \tau^{kj}(d_{rk}+\omega_{rk})g^{ri}.\end{aligned} \tag{67}$$

Taking advantage of the constitutive rate equation (57) and assuming that the constitutive response remains continuous at the inception of localization [*cf.* Rice (1977) and Rudnicki and Rice (1975)], then eqns (65)–(67) yield:

$$(n_i\mathbb{L}^{ijkl}n_k + A^{jl})k_l = 0, \tag{68}$$

where

$$A^{jl} = n_i\tau^{ik}n_k g^{jl}. \tag{69}$$

Substituting $\mathbb{L}$ from (58) into the fundamental condition (68) we obtain

$$\left[n_i \mathscr{L}^{e}{}_{ijkl} n_k - \frac{n_i \left(Q^{*ij} + \Theta \frac{z^{ij}}{\mu} \tau^{rs} N_{rs} \right) Q^{*kl} n_k}{h + Q^{*mn} N_{mn} + \left(\Theta \frac{z^{mn} N_{mn}}{\mu} - \Pi \right) \tau^{rs} N_{rs}} + A^{jl} \right] k_l = 0. \tag{70}$$

We shall follow here the procedure developed by Rice (1977) and Asaro and Rice (1977).

It is assumed that the inverse matrix $(\mathbf{n} \cdot \mathscr{L}^{e} \cdot \mathbf{n})^{-1}$ exists. Multiplying the last result by $(\mathbf{n} \cdot \mathscr{L}^{e} \cdot \mathbf{n})^{-1}$ we have, in abstract notation,

$$\left\{ \mathbf{I} + (\mathbf{n} \cdot \mathscr{L}^{e} \cdot \mathbf{n})^{-1} \cdot \mathbf{A} - \frac{(\mathbf{n} \cdot \mathscr{L}^{e} \cdot \mathbf{n})^{-1} \cdot \mathbf{n} \cdot \left(\mathbf{Q}^{*} + \Theta \frac{\mathbf{z}}{\mu} \tau : \mathbf{N} \right) \mathbf{Q}^{*} \cdot \mathbf{n}}{h + \mathbf{Q}^{*} : \mathbf{N} + \left(\Theta \frac{\mathbf{z} : N}{\mu} - \Pi \right) \tau : \mathbf{N}} \right\} \cdot \mathbf{k} = 0. \tag{71}$$

Since the term $(\mathbf{n} \cdot \mathscr{L}^{e} \cdot \mathbf{n})^{-1} \cdot \mathbf{A}$ is of the order of magnitude $(\tau / \mathscr{L}^{e})$ so it differs from the unit tensor only by $O(\tau / \mathscr{L}^{e})$-terms. Thus, we may assume that the tensor $[\mathbf{I} + (\mathbf{n} \cdot \mathscr{L}^{e} \cdot \mathbf{n})^{-1} \cdot \mathbf{A}]$ has an inverse and to calculate it to any desired degree of accuracy by the series, we obtain

$$[\mathbf{I} + (\mathbf{n} \cdot \mathscr{L}^{e} \cdot \mathbf{n})^{-1} \cdot \mathbf{A}]^{-1} = \mathbf{I} - (\mathbf{n} \cdot \mathscr{L}^{e} \cdot \mathbf{n})^{-1} \cdot \mathbf{A} + O\left(\frac{\tau^2}{\mathscr{L}^{e2}} \right). \tag{72}$$

When the previous result (71) is multiplied by this inverse, we have an expression in the form

$$\left[\mathbf{I} - \frac{\xi \zeta}{h + \mathbf{Q}^{*} : \mathbf{N} + \left(\Theta \frac{\mathbf{z} : \mathbf{N}}{\mu} - \Pi \right) \tau : \mathbf{N}} \right] \cdot \mathbf{k} = 0, \tag{73}$$

where

$$\xi = [\mathbf{I} + (\mathbf{n} \cdot \mathscr{L}^{e} \cdot \mathbf{n})^{-1} \cdot \mathbf{A}]^{-1} \cdot (\mathbf{n} \cdot \mathscr{L}^{e} \cdot \mathbf{n})^{-1} \cdot \left[\mathbf{n} \cdot \left(\mathbf{Q}^{*} + \Theta \frac{\mathbf{z}}{\mu} \tau : \mathbf{N} \right) \right],$$

$$\zeta = \mathbf{Q}^{*} \cdot \mathbf{n}. \tag{74}$$

Upon multiplying eqn (73) by ζ, we obtain

$$\left[1 - \frac{\zeta \cdot \xi}{h + \mathbf{Q}^{*} : \mathbf{N} + \left(\Theta \frac{\mathbf{z} : \mathbf{N}}{\mu} - \Pi \right) \tau : \mathbf{N}} \right] (\zeta \cdot \mathbf{k}) = 0. \tag{75}$$

In view of the fact that the term $\zeta \cdot \mathbf{k}$ cannot vanish for non-zero $\mathbf{k}$ unless the bifurcation mode $\mathbf{k}$ involves no plastic strain, the only relevant condition for non-zero $\mathbf{k}$ is

$$h + \mathbf{Q}^* : \mathbf{N} + \left(\Theta \frac{\mathbf{z} : \mathbf{N}}{\mu} - \Pi\right)\tau : \mathbf{N} = \zeta \cdot \xi. \tag{76}$$

This condition gives the critical h at macroscopic shear band localization as

$$h = \zeta \cdot \xi - \mathbf{Q}^* : \mathbf{N} - \left(\Theta \frac{\mathbf{z} : \mathbf{N}}{\mu} - \Pi\right)\tau : \mathbf{N}. \tag{77}$$

Substituting (56_1) and (69) into (74) and then (74) into (77) and estimating each term in this expression and neglecting terms of the order of magnitude (τ^2/μ^2) and $(\tau^2/\mu^2)\Theta$ in comparison to 1, we obtain

$$h(\mathbf{n}) = h_0(\mathbf{n}) + h_1(\mathbf{n}) + h_2(\mathbf{n}), \tag{78}$$

where

$$\begin{aligned}
h_0(\mathbf{n}) &= (\mathbf{N} : \mathscr{L}^e \cdot \mathbf{n}) \cdot (\mathbf{n} \cdot \mathscr{L}^e \cdot \mathbf{n})^{-1} \cdot (\mathbf{n} \cdot \mathscr{L}^e : \mathbf{N}) - \mathbf{N} : \mathscr{L}^e : \mathbf{N}, \\
h_1(\mathbf{n}) &= \Pi\tau - \Theta \frac{\tau}{\mu} \mathbf{z} : [\mathbf{N} - \mathbf{n}(\mathbf{n} \cdot \mathscr{L}^e \cdot \mathbf{n})^{-1} \cdot (\mathbf{n} \cdot \mathscr{L}^e : \mathbf{N})], \\
h_2(\mathbf{n}) &= 2[(\mathbf{n} \cdot \mathscr{L}^e \cdot \mathbf{n})^{-1} \cdot (\mathbf{n} \cdot \mathbf{b})] \cdot (\mathbf{n} \cdot \mathscr{L}^e : \mathbf{N}) \\
&\quad - [(\mathbf{n} \cdot \mathscr{L}^e \cdot \mathbf{n})^{-1} \cdot \mathbf{A}]^{-1} \cdot (\mathbf{n} \cdot \mathscr{L}^e \cdot \mathbf{n})^{-1} \cdot (\mathbf{n} \cdot \mathscr{L}^e : \mathbf{N}) \cdot (\mathbf{n} \cdot \mathscr{L}^e : \mathbf{N}) - \mathbf{b} : \mathbf{N}.
\end{aligned} \tag{79}$$

It is noteworthy to add that

$$\begin{aligned}
O\left(\frac{h_0}{\mu}\right) &= O(1), \\
O\left(\frac{h_1}{\mu}\right) &= O\left\{\max\left[\left(\Pi \frac{\tau}{\mu}\right), \left(\Theta \frac{\tau}{\mu}\right)\right]\right\}, \\
O\left(\frac{h_2}{\mu}\right) &= O\left(\frac{\tau}{\mu}\right).
\end{aligned} \tag{80}$$

The function h_0 describes the influence of the elastic–plastic properties of the crystal, h_1 represents the thermomechanical coupling effects (namely thermal plastic softening and thermal expansion) and h_2 encompasses the influence of the spatial covariance terms.

Let us consider the case $\mathbf{n} = \mathbf{m}$. Then we have

$$\begin{aligned}
h_0(\mathbf{m}) &= 0, \\
h_1(\mathbf{m}) &= \Pi\tau, \\
h_2(\mathbf{m}) &= \mathbf{N} : \mathbf{b} - \mathbf{s} \cdot \mathbf{A} \cdot \mathbf{s} = 0.
\end{aligned} \tag{81}$$

Thus, we have a very important result. When the plane of localization is either the slip plane, $\mathbf{n} = \mathbf{m}$, or the kink plane, $\mathbf{n} = \mathbf{s}$, it has been found that the critical plastic hardening modulus at the inception of localization is as follows:

$$h_{\text{crit}}(\mathbf{m}) = \Pi\tau. \tag{82}$$

To investigate the influence of the terms of the order of magnitude τ, $\Pi\tau$ and $\Theta\tau$ in eqn (78) we shall expand h in a series in $\mathbf{n}$, about $\mathbf{n} = \mathbf{m}$ (or $\mathbf{n} = \mathbf{s}$). In other words we shall apply the perturbation procedure about the slip (or kink)-plane orientation developed by Asaro and Rice (1977).

For the perturbation about $\mathbf{n} = \mathbf{m}$ we assume

$$\mathbf{n} = \mathbf{m} + \varepsilon, \tag{83}$$

where ε is understood to be small.

Expanding the expressions (79) in a series we find

$$\begin{aligned} h_0(\mathbf{n}) &= -\varepsilon \cdot (\mathbf{s} \cdot \mathscr{M} \cdot \mathbf{s}) \cdot \varepsilon + O(\mathscr{L}^e |\mathbf{n}-\mathbf{m}|^3), \\ h_1(\mathbf{n}) &= \Pi\tau + \Theta \frac{\tau}{\mu} \mathbf{z} : \mathscr{N} \cdot \varepsilon + O(\Pi\tau |\mathbf{n}-\mathbf{m}|^2, \Theta\tau |\mathbf{n}-\mathbf{m}|^2), \\ h_2(\mathbf{n}) &= 2\mathbf{s} \cdot \mathbf{b} \cdot \varepsilon - 2\mathbf{m} \cdot \tau \cdot \varepsilon + O(\tau |\mathbf{n}-\mathbf{m}|^2), \end{aligned} \tag{84}$$

where

$$\begin{aligned} \mathscr{M} &= \mathscr{L}^e - (\mathscr{L}^e \cdot \mathbf{m}) \cdot (\mathbf{m} \cdot \mathscr{L}^e \cdot \mathbf{m})^{-1} \cdot (\mathbf{m} \cdot \mathscr{L}^e), \\ \mathscr{N} &= \mathbf{s}\mathbf{1} - \mathbf{m}(\mathbf{m} \cdot \mathscr{L}^e \cdot \mathbf{m})^{-1} \cdot (\mathbf{m} \cdot \mathscr{L}^e \cdot \mathbf{m}). \end{aligned} \tag{85}$$

Since we do not know in advance the order of magnitude of ε, $\Pi\varepsilon$ and $\Theta\varepsilon$ in comparison to $\tau/\mathscr{L}^e$, we cannot be sure that the neglected terms in h_0, h_1 and h_2 are of the same order of magnitude.

Next, substituting $\mathbf{n}-\mathbf{m}$ for ε and combining (84) the expression (78) for the value of h at the localization on a plane having normal $\mathbf{n}$ may now be written in the form

$$\begin{aligned} h(\mathbf{n}) = &-(\mathbf{n}-\mathbf{m}) \cdot (\mathbf{s} \cdot \mathscr{M} \cdot \mathbf{s}) \cdot (\mathbf{n}-\mathbf{m}) + \Pi\tau + \Theta \frac{\tau}{\mu} \mathbf{z} : \mathscr{N} \cdot (\mathbf{n}-\mathbf{m}) \\ &+ 2\tau\mathbf{s} \cdot (\mathbf{n}-\mathbf{m}) + O(\mathscr{L}^e |\mathbf{n}-\mathbf{m}|^3, \Pi\tau |\mathbf{n}-\mathbf{m}|^2, \Theta\tau |\mathbf{n}-\mathbf{m}|^2, \tau |\mathbf{n}-\mathbf{m}|^2). \end{aligned} \tag{86}$$

Taking advantage of the discussion presented by Asaro and Rice (1977) which indicates that the inverse $(\mathbf{s} \cdot \mathscr{M} \cdot \mathbf{s})^{-1}$ exists, the orientation $\mathbf{n}$ which maximizes the right-hand side of (86) is as follows:

$$\mathbf{n} = \mathbf{m} + \tfrac{1}{2}\tau (\mathbf{s} \cdot \mathscr{M} \cdot \mathbf{s})^{-1} \cdot \left(\frac{\Theta}{\mu} \mathbf{z} : \mathscr{N} + 2\mathbf{s} \right), \tag{87}$$

where the terms of higher order of magnitude than $\tau/\mathscr{L}^e$ and $\Theta(\tau/\mathscr{L}^e)$ are neglected.

Substituting $\mathbf{n}$ given by (87) into (86) yields the critical hardening rate at the onset of localization:

$$h_{\text{crit}} = \Pi\tau + \tfrac{1}{4}\tau^2 \left(\frac{\Theta}{\mu} \mathbf{z} : \mathscr{N} + 2\mathbf{s} \right) \cdot (\mathbf{s} \cdot \mathscr{M} \cdot \mathbf{s})^{-1} \cdot \left(\frac{\Theta}{\mu} \mathbf{z} : \mathscr{N} + 2\mathbf{s} \right), \tag{88}$$

where again the terms of higher order of magnitude are neglected.

To obtain the direct analytical results we shall introduce the following simplifications:

(i) Let us assume [*cf.* Duszek and Perzyna (1991)]

$$\mathbf{z} = \mathbf{s} \cdot (\mathbf{s} \cdot \mathscr{L}^e). \tag{89}$$

(ii) Let us restrict our considerations to the linear, isotropic and homogeneous elastic properties of the crystal, i.e.

$$\mathscr{L}^{abcd} = \tau^{bd} g^{ac} + \mu (g^{ac} g^{bd} + g^{ad} g^{bc}) + \lambda g^{ab} g^{cd}, \tag{90}$$

where the constants μ and λ are the Lamé moduli.

Taking advantage of the simplification (89) we obtain

$$\mathbf{n} = \mathbf{m} + \tfrac{1}{2}\tau \frac{\Theta}{\mu}\mathbf{s} + \tau(\mathbf{s}\cdot\mathscr{M}\cdot\mathbf{s})^{-1}\cdot\mathbf{s}, \tag{91}$$

and

$$h_{\text{crit}} = \Pi\tau + \tfrac{1}{4}\tau^2\left[\frac{\Theta}{\mu}(\mathbf{s}\cdot\mathscr{M}\cdot\mathbf{s}) + 2\mathbf{g}\right]\cdot(\mathbf{s}\cdot\mathscr{M}\cdot\mathbf{s})^{-1}\cdot\left[\frac{\Theta}{\mu}(\mathbf{s}\cdot\mathscr{M}\cdot\mathbf{s}) + 2\mathbf{g}\right]. \tag{92}$$

Finally, introducing the simplification (90) we have

$$\mathbf{n} = \mathbf{m} + \frac{1}{4\nu}\frac{\tau}{\mu}(2\Theta\nu + 1)\mathbf{s} + O\left(\frac{\tau^2}{\mu}\right), \tag{93}$$

and

$$\left(\frac{h}{\tau}\right)_{\text{crit}} = \Pi + \frac{\tau}{\mu}\left(\Theta^2\nu + \Theta + \frac{1}{4\nu}\right) + O\left(\frac{\tau^2}{\mu}\right), \tag{94}$$

where

$$\nu = \frac{\lambda+\mu}{\lambda+2\mu}.$$

The results (93) and (94) are of sufficiently simple form to be used in qualitative analysis as well as in numerical estimations of the influence of the effects considered in shear band localization criteria.

A similar calculation can be carried out for the case in which the perturbation about the kink-plane $\mathbf{n} = \mathbf{s}$ is used. Then we write

$$\mathbf{n} = \mathbf{s} + \varepsilon. \tag{95}$$

The direction of the shear band at the inception of localization is as follows:

$$\mathbf{n} = \mathbf{s} + \frac{1}{4\nu}\frac{\tau}{\mu}(2\Theta\nu + 1)\mathbf{m} + O\left(\frac{\tau^2}{\mu}\right) \tag{96}$$

and the critical hardening rate is given by eqn (94).

It is noteworthy that the perturbation procedure used satisfies the requirement that $\mathbf{n}$, like $\mathbf{m}$, is a unit vector [*cf.* Asaro and Rice (1977)].

Indeed, since $\mathbf{m}\cdot\varepsilon = 0$ we have

$$\begin{aligned}\|\mathbf{n}\| &= [(\mathbf{m}+\varepsilon)\cdot(\mathbf{m}+\varepsilon)]^{1/2} = (\mathbf{m}\cdot\mathbf{m} + 2\mathbf{m}\cdot\varepsilon + \varepsilon\cdot\varepsilon)^{1/2} \\ &= (1 + \|\varepsilon\|^2)^{1/2} \approx 1.\end{aligned} \tag{97}$$

5. NUMERICAL ESTIMATIONS AND COMPARISON WITH EXPERIMENTAL RESULTS

5.1. *Numerical estimations*

In order to make numerical estimations of the results obtained let us write the final form for the strain-hardening modulus rate (94) as follows:

$$\left(\frac{h}{\tau}\right)_{\text{crit}} = \Pi + \left(\frac{\tau}{\mu}\right)_{\text{crit}}\left(\nu\Theta^2 + \Theta + \frac{1}{4\nu}\right) \tag{98}$$

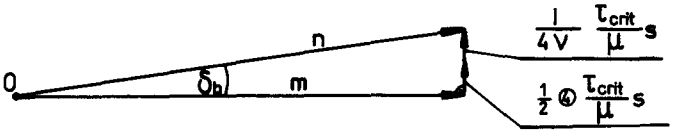

Fig. 8. Theoretical approximation of the misalignment of the direction of the macroscopic shear band **n** from active slip systems in the crystal's matrix.

and approximate (93) by (*cf.* Fig. 8)

$$\mathbf{n} = \mathbf{m} + \tfrac{1}{2}\left(\frac{\tau}{\mu}\right)_{\text{crit}}\left(\Theta + \frac{1}{2v}\right)\mathbf{s}. \tag{99}$$

The numerical computations are obtained for Al–Cu single crystals and for nitrogenated Fe–Ti–Mn single crystals. Some particular material parameters are taken from Chang and Asaro's (1981) and Spitzig's (1981) experimental data. All other parameters are as given in Table 1.

(i) *Aluminum–copper single crystals tested at* 298K. The following parameters have been taken from Chang and Asaro's (1981) experimental data:

$$\left(\frac{\tau}{\mu}\right)_{\text{crit}} = 7.5\times 10^{-3}, \quad \frac{\partial \tau_{\text{crit}}}{\partial \vartheta} = -0.06\times 10^{6}\,\text{Pa K}^{-1}.$$

Equation (98) gives

$$\left(\frac{h}{\tau}\right)_{\text{crit}} = 0.0235+0.0004+0.0018+0.0025 = 0.0282.$$

Equation (99) yields

$$\mathbf{n} = \mathbf{m} + (0.0009+0.0025)\mathbf{s},$$

and

$$\tan\delta_b = 0.0034 \Rightarrow \delta_b = 12'.$$

(ii) *Aluminum–copper single crystals tested at* 77K. Again from Chang and Asaro's (1981) experimental data we have

$$\left(\frac{\tau}{\mu}\right)_{\text{crit}} = 1.5\times 10^{-2}, \quad \frac{\partial \tau_{\text{crit}}}{\partial \vartheta} = -0.08\times 10^{6}\,\text{Pa K}^{-1},$$

Table 1. Material parameters

	Parameter	Unit	Aluminium	Iron
ρ	Density	Kg m^{-3}	2702	7850
c_p	Specific heat	$\text{J Kg}^{-1}\text{K}^{-1}$	896	465
μ	Shear modulus	GPa	26.0	82.0
E	Young's modulus	GPa	71.0	210.0
K	Bulk modulus	GPa	73.2	170.0
θ	Coefficient of thermal expansion	K^{-1}	23.8×10^{-6}	12.1×10^{-6}
	χ	—	0.85–0.95	

and

$$\left(\frac{h}{\tau}\right)_{\text{crit}} = 0.0314+0.0007+0.0036+0.0050 = 0.0407,$$

$$\mathbf{n} = \mathbf{m}+(0.0018+0.0050)\mathbf{s},$$

$$\tan\delta_h = 0.0068 \Rightarrow \delta_h \approx 23'.$$

(iii) *Nitrogenated Fe–Ti–Mn single crystals tested at* 295K. From Spitzig's (1981) experimental data:

$$\left(\frac{\tau}{\mu}\right)_{\text{crit}} = 0.855\times 10^{-2}, \quad \tau_{\text{crit}} = 701.10\times 10^{6}\ \text{Pa},$$

$$\frac{\partial\tau_{\text{crit}}}{\partial\vartheta} = -0.15\times 10^{6}\ \text{Pa K}^{-1},$$

then

$$\left(\frac{h}{\tau}\right)_{\text{crit}} = 0.0390+0.005+0.0022+0.0030 = 0.0447$$

or

$$h_{\text{crit}} = 31.34\,\text{MPa},$$

while

$$\mathbf{n} = \mathbf{m}+(0.0011+0.0030)\mathbf{s},$$

and

$$\tan\delta_h = 0.0041 \Rightarrow \delta_h \approx 15'.$$

5.2. *Comparison with experimental results*

Let us first make a comparison between the theoretical predictions for $(h/\tau)_{\text{crit}}$ for aluminum–copper single crystals and the experimental results obtained by Chang and Asaro (1981). The critical ratio $(h/\tau)_{\text{crit}}$ versus the angle between the tensile axis and $\bar{1}12$ for various ageing treatments obtained by Chang and Asaro (1981) is plotted in Fig. 2. It seems that the comparison of the theoretical predictions estimated in Section 5.1 with the Chang and Asaro experimental results is extremely good.

A similar conclusion can be drawn from the comparison of Spitzig's (1981) experimental results for nitrogenated Fe–Ti–Mn crystals with the theoretical predictions obtained in Section 5.1.

Spitzig's experimental data are as follows:

$$(h/\tau)_{\text{crit}} = 0.03\div 0.06 \quad \text{or} \quad h_{\text{crit}} = 25\div 45\,\text{MPa},$$

while the theoretical results read:

$$(h/\tau)_{\text{crit}} = 0.0447 \quad \text{or} \quad h_{\text{crit}} = 31.34\,\text{MPa}.$$

To compare the theoretical predictions for the misalignment of the direction of the macroscopic shear band from the active slip systems in the crystal's matrix we first take into account that the theoretical estimations concerned the angle δ_h, i.e. at the inception of the shear band localization, while the experimental observations of the misalignment performed by Chang and Asaro (1981) for aluminum–copper single crystals and by Spitzig (1981) for nitrogenated Fe–Ti–Mn crystals have been detected at the end of the process considered, i.e. at the point (c) as has been explained in Fig. 7.

This interpretation of the experimental observations helps us to draw the conclusion that the description of the misalignment by incorporating the synergetic effects resulting from simultaneous consideration of the spacial covariance effects and thermomechanical couplings (as has been estimated in Section 5.1) is realistic and looks promising.

6. DISCUSSION OF THE RESULTS

6.1. *Thermal effects*

There are two thermal effects which influence the criteria for adiabatic shear band localization, namely thermal expansion and thermal plastic softening.

Thermal expansion affects the critical hardening rate $(h/\tau)_{\text{crit}}$ [*cf.* eqn (98)], as well as the direction of the shear band $\mathbf{n}$ [*cf.* eqn (99)], while thermal plastic softening influences only the critical hardening rate $(h/\tau)_{\text{crit}}$.

The contribution to the critical hardening rate generated by thermal expansion is small and consists of two terms: $2(\tau/\mu)_{\text{crit}}\nu\Theta^2$ and $2(\tau/\mu)_{\text{crit}}\Theta$. The first term is five times smaller than the second which has a synergetic nature. The second term represents the cooperative phenomena of thermal expansion and spatial covariance effects.

The main contribution to the critical hardening rate is implied by thermal plastic softening represented by Π. This term dominates the result and is of the order of 10^{-2} while the thermal expansion term is of the order of 10^{-4}.

6.2. *Misalignment of the shear bands*

The misalignment of the direction of the macroscopic shear bands from the active slip systems in the crystal's matrix is affected by two phenomena, namely by thermal expansion and spatial covariance effects.

The spatial covariance term

$$\frac{1}{4\nu}(\tau/\mu)_{\text{crit}}$$

has dominated influence on the direction of the shear band and is 2.5 times larger than the thermal expansion term $\frac{1}{2}\Theta(\tau/\mu)_{\text{crit}}$.

The theoretical results for the angle δ_b at the inception of the shear band localization have been estimated in Section 5 for aluminum–copper single crystals tested at 298 and 77K and for nitrogenated Fe–Ti–Mn single crystals tested at 295K. It has been found that obtained values of the angle δ_b are small but sufficiently distinct to explain the experimentally observed misalignment.

6.3. *Spatial covariance effects*

To make estimations of the influence of the spatial covariance terms on shear band localization conditions let us assume an isothermal process, then $\Theta = 0$ and $\Pi = 0$, and eqns (98) and (99) yield

$$\left(\frac{h}{\tau}\right)_{\text{crit}} = \left(\frac{\tau}{\mu}\right)_{\text{crit}} \frac{1}{4\nu}, \tag{100}$$

$$\mathbf{n} = \mathbf{m} + \left(\frac{\tau}{\mu}\right)_{\text{crit}} \frac{1}{4\nu}\mathbf{s}. \tag{101}$$

Numerical estimations are as follows:

(i) Aluminum–copper single crystals tested at 298K:

$$\left(\frac{h}{\tau}\right)_{\text{crit}} = 0.0025,$$

$$\mathbf{n} = \mathbf{m} + 0.0025\mathbf{s}, \quad \tan\delta_b = 0.0025 \Rightarrow \delta_b \approx 9'.$$

(ii) Aluminum–copper single crystals tested at 77K:

$$\left(\frac{h}{\tau}\right)_{\text{crit}} = 0.0050,$$

$$\mathbf{n} = \mathbf{m} + 0.0050\mathbf{s}, \quad \tan\delta_h = 0.0050 \Rightarrow \delta_h = 17.5'.$$

(iii) Nitrogenated Fe–Ti–Mn single crystals tested at 295K:

$$\left(\frac{h}{\tau}\right)_{\text{crit}} = 0.0030 \quad \text{or} \quad h_{\text{crit}} = 2.1\,\text{MPa},$$

$$\mathbf{n} = \mathbf{m} + 0.0030\mathbf{s}, \quad \tan\delta_h = 0.0030 \Rightarrow \delta_h = 11'.$$

Based on these numerical estimations we may conclude that theoretical values obtained for the critical hardening rate $(h/\tau)_{\text{crit}}$ are too small when compared with experimental results. Indeed, an obtained value of $(h/\tau)_{\text{crit}}$ is of the order 10^{-3}, while the expected result is of the order of 10^{-2}.

However, an analysis of the theoretical results concerning the predicted direction of the macroscopic shear bands allows us to draw the conclusion that the spatial covariance effects play a very important role in the description of the misalignment of the shear bands from the active slip systems in the crystal's matrix.

6.4. *Non-Schmid effects*

Let us consider small departures from the Schmid description as have been suggested by Asaro and Rice (1977), i.e. in the sense that stress increment components other than $d\tau_{ms}$ affect the shear $d\gamma$, and may be important to the explanation of critical conditions for localization.

Then the yield criterion takes the form

$$\tau - \boldsymbol{\alpha} : \boldsymbol{\tau} = \tau_c(\gamma, \vartheta), \tag{102}$$

where $\boldsymbol{\alpha}$ denotes the symmetric tensor of non-Schmid effects. It is assumed that $\boldsymbol{\alpha}$ is constant in time and is of the order of $\tau/\mathscr{L}^e$.

Differentiation of (102) with respect to time gives

$$\dot{\gamma} = \frac{1}{h}(\dot{\tau} + \boldsymbol{\alpha} : \dot{\boldsymbol{\tau}}) + \pi\dot{\vartheta}. \tag{103}$$

Replacing $\dot{\tau}$ by (52) and $\dot{\boldsymbol{\tau}} : \boldsymbol{\alpha}$ by

$$\begin{aligned}\dot{\boldsymbol{\tau}} : \boldsymbol{\alpha} &= (\overset{\text{el}}{\dot{\boldsymbol{\tau}}} : \boldsymbol{\alpha}) = (\overset{\text{el}}{\mathbf{L}}_{\text{v}})(\boldsymbol{\tau} : \boldsymbol{\alpha}) \\ &= (\overset{\text{el}}{\mathbf{L}}_{\text{v}}) : \boldsymbol{\alpha} - \boldsymbol{\tau} : [(\mathbf{d}^e + \boldsymbol{\omega}^e) \cdot \boldsymbol{\alpha} + \boldsymbol{\alpha} \cdot (\mathbf{d}^e + \boldsymbol{\omega}^e)] \\ &\approx (\overset{\text{el}}{\mathbf{L}}_{\text{v}}) : \boldsymbol{\alpha} \approx (\mathscr{L}^e : \mathbf{d}^e) : \boldsymbol{\alpha}\end{aligned} \tag{104}$$

we obtain

$$\dot{\gamma} = \frac{(\mathbf{Q}^* + \mathscr{L}^e : \boldsymbol{\alpha}) : \mathbf{d}}{h - \boldsymbol{\Pi}\tau : \mathbf{N} + \left(\mathbf{Q}^* + \frac{\Theta}{\mu}\tau : \mathbf{N}\mathbf{z} + \mathscr{L}^e : \boldsymbol{\alpha}\right) : \mathbf{N}}. \tag{105}$$

The fundamental rate equation for the Kirchhoff stress tensor τ finally has the form

$$L_v\tau = \mathbb{L}^* : \mathbf{d}, \tag{106}$$

where

$$\mathbb{L}^* = \left[\mathscr{L}^e - \frac{\left(\mathbf{Q}^* + \frac{\Theta}{\mu}\mathbf{z}\tau : \mathbf{N} + \mathscr{L}^e : \boldsymbol{\alpha}\right)\mathbf{Q}^*}{h - \boldsymbol{\Pi}\tau + \left(\mathbf{Q}^* + \frac{\Theta}{\mu}\mathbf{z}\tau : \mathbf{N} + \mathscr{L}^e : \boldsymbol{\alpha}\right) : \mathbf{N}}\right]. \tag{107}$$

For the perturbation about $\mathbf{n} = \mathbf{m}$ we obtain the orientation $\mathbf{n}$ which maximizes the hardening rate in the form

$$\mathbf{n} = \mathbf{m} + \tfrac{1}{2}(\mathbf{s}\cdot\mathscr{M}\cdot\mathbf{s})^{-1}\left[\left(\frac{\Theta}{\mu}\mathbf{z} : \mathscr{N} + 2\mathbf{s}\right)\tau + \mathbf{s}\cdot\mathscr{M} : \boldsymbol{\alpha}\right] + O(\alpha^2, \tau/\mathscr{L}^e) \tag{108}$$

and the critical hardening rate at the onset of shear band localization is as follows:

$$h_{\text{crit}} = \boldsymbol{\Pi}\tau + \tfrac{1}{4}\left(\Theta\frac{\tau}{\mu}\mathbf{z} : \mathscr{N} + 2\tau\mathbf{s} + \boldsymbol{\alpha} : \mathscr{M}\cdot\mathbf{s}\right)\cdot(\mathbf{s}\cdot\mathscr{M}\cdot\mathbf{s})^{-1} \cdot\left(\Theta\frac{\tau}{\mu}\mathbf{z} : \mathscr{N} + 2\tau\mathbf{s} + \mathbf{s}\cdot\mathscr{M} : \boldsymbol{\alpha}\right) + O(\alpha\tau, \tau/\mathscr{L}^e, \alpha^3\mathscr{L}^e). \tag{109}$$

Taking advantage of the simplifications (89) and (90) we obtain

$$\mathbf{n} = \mathbf{m} + \frac{1}{2}\Theta\frac{\tau}{\mu}\mathbf{s} + \frac{1}{4}\frac{\tau}{\mu}\frac{1}{\nu}\mathbf{s} + \alpha_{zs}\mathbf{z} + \frac{1}{4\nu}[(2\nu - 1)\alpha_{zs} + 2\nu\alpha_{ss}]\mathbf{s},$$

$$h_{\text{crit}} = \boldsymbol{\Pi}\tau + \frac{1}{4\nu\mu}[2\Theta\tau\nu + \tau + \mu(2\nu - 1)\alpha_{zz} + 2\mu\nu\alpha_{ss}] + \mu\alpha_{zs}^2. \tag{110}$$

Assuming the particular case when $\alpha_{sz} = \alpha_{zs} = \frac{1}{2}\alpha$, $\alpha_{zz} = \alpha_{ss} = 0$ we have

$$\mathbf{n} = \mathbf{m} + \frac{1}{4\nu}\frac{\tau}{\mu}(2\Theta\nu + 1)\mathbf{s} + \frac{1}{2}\alpha\mathbf{z},$$

$$\left(\frac{h}{\tau}\right)_{\text{crit}} = \boldsymbol{\Pi} + \frac{\tau}{\mu}\left(\Theta^2\nu + \Theta + \frac{1}{4\nu}\right) + \frac{1}{4}\alpha^2\frac{\mu}{\tau}. \tag{111}$$

Using the Zaremba–Jaumann rate instead of the Lie derivative and assuming an isothermal process then eqns (105)–(111) reduce to those obtained first by Asaro and Rice (1977).

Asaro and Rice (1977) also introduced a dislocation model for non-Schmid effects at the onset of cross-slip in f.c.c. crystals. They estimated some of the continuum parameters on which h_{crit} is found to depend. However, their estimations were obtained under the very strong assumption that h_{crit} is affected only by non-Schmid effects.

If we take into consideration the fact that h_{crit} is affected by several effects, such as thermal plastic softening, thermal expansion, spatial covariance, non-Schmid and some synergetic interactions then final estimations for non-Schmid parameters have to be smaller than those obtained by Asaro and Rice (1977).

6.5. *Localization modes*

As has been shown by experimental investigations, in general during the uniaxial tension test the localization by necking mode proceeds the localization by adiabatic shear band forming mode. This fact may have very important consequences for the determination of the shear band localization criteria.

Indeed, at the stage of the tensile process when the load–engineering strain trajectory reaches its maximum, i.e. when the criterion for the onset of the localization by necking mode is satisfied a crystal specimen exhibits diffuse necking. This is a very important stage of the tensile process when the gross plastic deformations are localized to the diffusely necked region and the state of stress is no longer homogeneous. An inhomogeneous distribution of stress in the necked region is found to affect the adiabatic shear band localization criteria.

However, this fact has not been taken into consideration in our procedure developed in Section 4.

The fundamental assumption of our considerations is that the boundary conditions are such that a body sustains a uniform distribution of stress as well as temperature.

This needs further careful analysis and investigations into how the criteria for shear band localization can be affected by a non-uniform distribution of stress within the necked region.

7. FINAL COMMENTS

The thermomechanical theory of shear band localization of single crystals presented in this paper has been inspired by the theoretical work by Asaro and Rice (1977) and by the experimental investigations performed by Chang and Asaro (1981) and Spitzig (1981). These theoretical and experimental works have brought deep understanding of shear band localization conditions for elastic–plastic single crystals in isothermal processes.

The main purpose of this paper is the investigation of shear band localization criteria for elastic–plastic single crystals in adiabatic processes. The examination of two important thermal effects, namely thermal expansion and thermal softening, is presented. It has been proved that thermal expansion influences mainly the description of the misalignment of the direction of the macroscopic shear bands from the active slip systems in the crystal's matrix, while thermal plastic softening has dominated influence only on the critical hardening rate.

The second objective is the investigation of the influence of spatial covariance terms. It has been found that the spatial covariance effects play a very important role in the description of the misalignment of the shear bands from the active slip systems.

Numerical estimations have proved that by incorporating the thermomechanical effects and spatial covariance effects in a constitutive law of elastic–plastic single crystals the critical hardening rate h_{crit} at the inception of localization is small but positive. The computed critical value of the strain hardening rate h_{crit} as well as the difference between the direction of the macroscopic shear band and the primary slip systems of the single crystal appeared to be in accord with the experimental results of Chang and Asaro (1981) for Al–Cu single crystals and Spitzig (1981) for Fe–Ti–Mn single crystals.

A discussion of small departure from the Schmid description [as first suggested by Asaro and Rice (1977)] is also presented. It has been shown that since h_{crit} is affected by several effects such as thermal plastic softening, thermal expansion, spatial covariance, non-Schmid and some synergetic interactions, then final estimations for non-Schmid parameters have to be smaller than those found by Asaro and Rice (1977).

It has been noted that rate sensitivity effects need further investigations.

REFERENCES

Abraham, R., Marsden, J. E. and Ratiu, T. (1988). *Manifolds, Tensor Analysis and Applications*. Springer, Berlin.
Asaro, R. J. (1983a). Micromechanics of crystals and polycrystals. *Advances Appl. Mech.* **23**, 1–115.

Asaro, R. J. (1983b). Crystal plasticity. *J. Appl. Mech.* **50,** 921–934.
Asaro, R. J. and Needleman, A. (1985). Texture development and strain hardening in rate dependent polycrystals. *Acta Metall.* **33,** 923–953.
Asaro, R. J. and Rice, J. R. (1977). Strain localization in ductile single crystals. *J. Mech. Phys. Solids* **25,** 309–338.
Chang, Y. W. and Asaro, R. J. (1980). Lattice rotations and localized shearing in single crystals. *Arch. Mech.* **32,** 369–388.
Chang, Y. W. and Asaro, R. J. (1981). An experimental study of shear localization in aluminum–copper single crystals. *Acta Metall.* **29,** 241–257.
Chin, G. Y., Hosford, W. F. and Backofen, W. A. (1964). *Trans. ASME* **230,** 437.
Duszek, M. K. and Perzyna, P. (1991). The localization of plastic deformation in thermoplastic solids. *Int. J. Solids Structures* **27,** 1419–1443.
Havner, K. S. and Shalaby, A. M. (1977). A simple mathematical theory of finite distortional latent hardening in single crystals. *Proc. R. Soc. London* **A358,** 47–70.
Hill, R. (1966). Generalized constitutive relations for incremental deformation of metals crystals by multislip. *J. Mech. Phys. Solids* **14,** 95–102.
Hill, R. (1967). The essential structure of constitutive laws for metal composites and polycrystals. *J. Mech. Phys. Solids* **15,** 79–95.
Hill, R. (1972). On constitutive macro-variables for heterogeneous solids at finite strain. *Proc. R. Soc. London* **A326,** 131–147.
Hill, R. and Rice, J. R. (1972). Constitutive analysis of elastic–plastic crystals at arbitrary strain. *J. Mech. Phys. Solids* **20,** 401–413.
Hill, R. and Rice, J. R. (1973). Elastic potentials and the structure of inelastic constitutive laws. *SIAM J. Appl. Math.* **25,** 448–461.
Hutchinson, J. W. (1970). Elastic–plastic behaviour of polycrystalline metals and composites. *Proc. R. Soc. London* **A319,** 247–272.
Hutchinson, J. W. (1976). Bounds and self-consistent estimates for creep of polycrystalline materials. *Proc. R. Soc. London* **A348,** 101–127.
Iwakuma, T. and Nemat-Nasser, S. (1984). Finite elastic–plastic deformation of polycrystalline metals. *Proc. R. Soc. London* **A394,** 87–119.
Marsden, J. E. and Hughes, T. J. R. (1983). *Mathematical Foundations of Elasticity.* Prentice-Hall, Englewood Cliffs, NJ.
Nemat-Nasser, S. and Obata, M. (1986). Rate-dependent, finite elasto–plastic deformation of polycrystals. *Proc. R. Soc. London* **A407,** 343–375.
Oldroyd, J. (1950). On the formulation of rheological equations of state. *Proc. R. Soc. London* **A200,** 523–541.
Peirce, D., Asaro, R. J. and Needleman, A. (1982). An analysis of nonuniform and localized deformation in ductile single crystals. *Acta Metall.* **30,** 1087–1119.
Peirce, D., Asaro, R. J. and Needleman, A. (1983). Material rate dependence and localized deformation in crystalline solids. *Acta Metall.* **13,** 1951–1976.
Perzyna, P. (1988). Temperature and rate dependent theory of plasticity of crystalline solids. *Rev. Phys. Appl.* **23,** 445–459.
Perzyna, P. (1990). Constitutive equations of dynamic plasticity. In *Enelastic Solids and Structures. A. Sawczuk Memorial Volume* (Edited by M. Kleiber and J. A. König), pp. 111–129. Pineridge Press, Trowbridge.
Rice, J. R. (1971). Inelastic constitutive relations for solids: an internal-variable theory and its application to metal plasticity. *J. Mech. Phys. Solids* **19,** 443–455.
Rice, J. R. (1977). The localization of plastic deformation. In *Proc. 14th Int. Congress of Theo. Appl. Mech. I,* (Edited by W. T. Koiter), pp. 207–220. North-Holland, Amsterdam.
Rudnicki, J. W. and Rice, J. R. (1975). Conditions for the localization of deformation in pressure-sensitive dilatant materials. *J. Mech. Phys. Solids* **23,** 371–394.
Schmid, E. (1924). *Proc. First Int. Congr. Appl. Mech.* (Edited by J. M. Biezeno), p. 342. Tech. Boekhandel, Delft.
Spitzig, W. A. (1981). Deformation behavior of nitrogenated F_e–T_i–M_n and F_e–T_i single crystals. *Acta Metall.* **29,** 1359–1377.
Su, X. M. and Lu, W. D. (1991). On the strain localization of ductile single crystals undergoing single slip. *Int. J. Solids Structures* **27,** 49–58.
Truesdell, C. and Noll, W. (1965). The non-linear field theories of mechanics. In *Handbuch der Physik* (Edited by S. Flügge), Vol. III/3, pp. 1–579. Springer, Berlin.